Available online at www.sciencedirect.com

ScienceDirect

Energy Procedia 80 (2015) 255 – 262

Energy Procedia

12th Deep Sea Offshore Wind R&D Conference, EERA DeepWind'2015

Coupled mooring systems for floating wind farms

Marek Goldschmidt*, Michael Muskulus

Department of Civil and Transport Engineering, Norwegian University of Science and Technology, Høgskoleringen 7A, 7491 Trondheim, Norway

Abstract

In this paper it is investigated if, by coupling the catenary mooring systems of a number of turbines, the number of lines and anchors needed and subsequently the costs could be reduced and what kind of dynamic phenomena such a mooring system will exhibit. A row, triangular and rectangular arrangement of floating wind turbines is analyzed in terms of their cost saving potential and their dynamic properties in the frequency domain. The row arrangement is further investigated in the time domain, with a one dimensional simplified model. The most important forces to evaluate the station keeping performance, except current, are applied. These consist of irregular wave forces, employing the Morison equation, estimated wave drift and wind forces. Diffraction effects have been estimated by employing the McCamy-Fuchs theory. Four operational and a 50-year extreme load case have been applied. The results are showing that significant cost reductions of up to 60% in mooring system and 8% in total system costs could be achieved. The dynamic analysis shows the general feasibility of integrated mooring systems. No resonance problems seem to exist. However displacements are increasing with the number of floaters, and cost savings diminish for larger numbers of turbines, as the required diameters, lengths and costs of mooring chains increase.

Peer-review under responsibility of SINTEF Energi AS

Keywords: Coupled mooring system, Frequency domain, Time domain, Catenary, Floating wind turbines, Semi-submersible

1. Introduction

At sites with very high water depths traditional support structures for offshore wind turbines such as monopiles, jackets, tripods, or tripiles suffer from unfavorable economic performance. The concept of floating offshore wind turbines (FOWT) seems to be an appropriate solution. However, the mooring system incurs a significant cost. It is

* Corresponding author. Tel.: +49-1577-1954170.
E-mail addresses: goldschmidtmarek@gmail.com (Marek Goldschmidt), michael.muskulus@ntnu.no (Michael Muskulus)

Peer-review under responsibility of SINTEF Energi AS
doi:10.1016/j.egypro.2015.11.429

therefore interesting to study if, by coupling the individual catenary mooring systems of a number of turbines, the number of lines and anchors needed and subsequently the cost could be reduced. The aim is to understand the potential cost reductions and what kind of dynamic phenomena such a mooring system will exhibit. In this work a semi-submersible floater equipped with a wind turbine will be used as example. The dynamics of semi-submersibles and catenary mooring systems are well known from the oil & gas industry and described by e.g. Barltrop [1], Chakrabarti [2] and Faltinsen [4]. An integrated mooring system has been investigated by Gao & Moan in [7], where multiple floating wave energy converters were moored using taut lines with buoys. Oceanwind Technology LLC has described coupled mooring systems for floating offshore wind farms in their patent [11]. Fredriksson et al. used an integrated mooring system in [6], where numerical modeling techniques for large fish farms are studied and compared to mooring tension measurements.

Mooring systems provide station keeping for floating offshore wind turbines, by keeping the translational motions in surge & sway and the rotational motions in yaw within the specified limits. To evaluate the feasibility of a mooring system design, the station keeping performance is therefore an important criterion. In this work only translational motions in surge and sway are considered, yaw motions are neglected.

Different wind farm layouts (row, rectangular and triangular arrangements, see Fig. 1 a-c, respectively), are analyzed in terms of their dynamic properties in the frequency domain and their cost saving potential. The row arrangement, simplified as a one dimensional system, has been further investigated in the time domain. Two coupled row-configurations with 5 and 10 FOWTs in a row are studied and compared to each other and a traditional moored turbine, with 2 anchor lines.

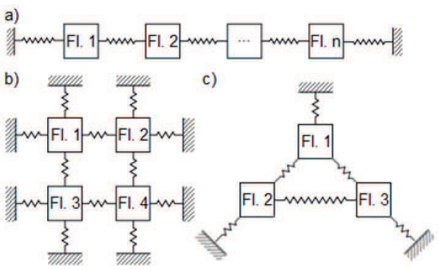

Fig. 1. Wind farm layouts: a) row, b) rectangular, c) triangular

2. Implementation

2.1. Floater and mooring systems

In this work the “DeepC” semi-submersible floating offshore wind turbine from phase II of the OC4 project is used as an example [8]. A NREL 5 MW baseline wind turbine is based on a main column, which is centered between three offset columns. The dimensions and properties of the structure are shown in Table 1 and Fig. 2. For simplification the braces are ignored and the diameter of the offset columns is assumed to be solely 12m, including the base columns. Even so the floater is designed to have a mooring system setup of three lines, one line connected to each of the three offset columns; it is also used with two and four mooring lines in this work. It is an adequate approach to compare different mooring system layouts, as only the total system dynamic is to be studied and yaw rotations are ignored. The mooring system properties of three investigated layouts are shown in Table 2; note that some properties are only valid for configurations with 2 row, 3 triangular and 4 rectangular arranged FOWTs. An anchored line is connected with one end to a floater and the other end to an anchor at the seabed. Two neighboring floaters are connected via a somewhat shorter line that is freely hanging (termed coupled line in Table 2).

Table 1. Floater properties

FOWT system mass [kilotons]	13.47
Draft [m]	20
Depth to fairleads below SWL [m]	14
Elevation of offset columns above SWL [m]	12
Diameter of main column [m]	6.5
Diameter of upper offset columns [m]	12

Table 2. Mooring system properties

Floater arrangement	row	triangular	rectangular
Water depth [m]	200	200	200
Number of lines connected to FOWT	2	3[1]	4
Angle between adjacent lines [deg]	180	various	90
Anchored/coupled line length [m]	835.7[1]/677.9[1]	838.1[1]/677.9[1]	835.7[1]/677.9[1]
Anch./coupl. horizontal distance [m]	792.9[1]/640.0[1]	794.3[1]/640.0[1]	792.9[1]/640.0[1]
Diameter of mooring chain [mm]	92[1]	100.2[1]	92[1]
Mass of chain [kg/m]	156.9[1]	185.0[1]	156.9[1]

[1]only valid for the smallest possible coupled setups (2 in a row, 3 triangular & 4 rectangular)

2.2. Environmental loading

In this work a site in the North-Sea is chosen as example. Only wind and wave loads are applied. Operational load cases 1-4 shown in Table 3 are taken from the UpWind design base [5], which represent typical environmental loads for a deep water offshore site in the North-Sea. Additionally a 50-year extreme wave load case from the phase II of the OC4 project [8] has been applied, to investigate the performance of integrated mooring systems under extreme conditions.

Table 3. Applied load cases

LC	v (m/s)	TI (%)	H_S (m)	T_P (s)	Peakedness γ	occ./year (hrs)
1	6	17.5	1.18	5.76	3.3	1230.6
2	12	14.6	1.70	5.88	3.3	1121.8
3	18	13.6	2.47	6.71	3.3	427.3
4	24	13.1	3.42	7.80	3.3	85.6
5	24	13.1	15.0	19.2	3.3	50-year event

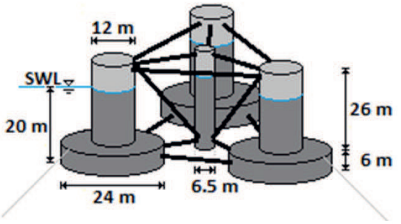

Fig. 2. DeepC semi-submersible floating wind turbine from phase II. of OC4

2.3. Modeling approach

The dynamic behavior is analyzed employing a standard equation of rigid body motion [1, eq. 5.1] which is modified for the application in hydrodynamics and solved in both frequency and time domain. The catenary mooring system is modeled using the catenary equation [4, eq. 8.21]. For calculations in the frequency domain the mooring system is simplified by a linearized stiffness matrix. For the solution in the time domain a quasi-static catenary model is used which is coupled to the overall hydrodynamic analysis to solve to the response of the floater [2]. In the time domain, the most important forces to evaluate the station keeping performance of mooring systems, except current are applied [9]. Linear wave theory with Wheeler stretching is used to determine the wave kinematics for the irregular wave forces. Five load cases as listed in Table 3 have been applied, using the stated parameters with JONSWAP wave spectra. The first order wave forces have been calculated using the Morison equation for a moving body including the added mass term and the relative velocity viscous drag term with damping. Numerical diffraction theory was not applied and radiation damping has been neglected as the diffraction parameter was mostly below 0.2. However, at lower wave heights and periods, diffraction parameters above 0.2 occur. Therefore diffraction effects have been estimated by employing McCamy-Fuchs theory. Second order slow drift forces are important to consider, as their excited motions lie in the resonance range of moored structures. Mean drift and slowly varying drift forces are determined employing Newman's approximation [4]. The transfer function T_{jj}^{ic} for the calculation is estimated by using values for fixed cylinders proposed by Chakrabarti [3], shown in Fig. 3. Wind forces are represented by wind thrust force time series from an uncoupled NREL 5 MW baseline turbine, hence dynamic interactions between rotor, nacelle and substructure, incl. floater, are not considered.

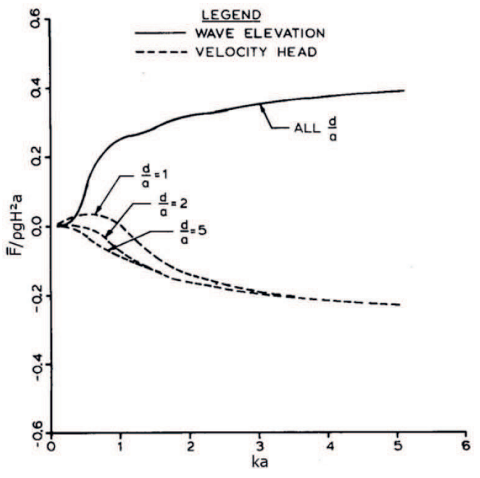

Fig. 3. Mean potential drift force on a fixed vertical cylinder in deep water, where a is the radius [3]

3. Results

3.1. Dynamic properties of the different layouts

The eigenvalues of the row, triangular and rectangular layouts as stated in Table 2 were studied in the frequency domain. The analysis has not indicated any problematic dynamic behavior as natural periods were far above first-order wave periods hence no

resonance would occur. The smallest natural periods found in this analysis were 60s or above for the different investigated layouts.

3.2. Time domain analysis of one dimensional coupled row arranged wind farms

In a simplified approach the row-arranged layout is considered a one-dimensional system, where the forces are acting in line with the row-/x-axis. This simplification disregards loads that come at an angle and the corresponding displacements in the 2-d-water-plane, which may be critical for this mooring system layout. However this layout is not considered a real world solution, as opposed to the triangular and rectangular layouts, but the simplified analysis of it is assumed to give a first understanding of what dynamic phenomena coupled mooring systems may exhibit and if system cost reductions can be achieved.

Analysis in the time domain was performed with simulation times of 840s, where the first 240s are cut off to remove transient effects. Adequate mooring system configurations for each row arrangement, with 5 & 10 coupled FOWTs and a single FOWT setup were found, which are displayed in Table 4, using the critical 50-year extreme wave load case (LC5) considering maximal allowed relative displacements, where mooring lines do not become taut and the breaking strength of the chains, assuming grade R4 is not exceeded. The dynamic responses of the found mooring system configurations to load case 5 are compared in the following section. For better visibility results for only the two outside floaters and a single internal floater is shown in some cases. In Fig. 4 displacement time series of the three mooring system configurations are shown in the first row. The corresponding power spectral densities

Table 4. Row arranged mooring system configurations for a single & coupled FOWTs

Number of FOWT in a row	1	5	10
Anchored/coupled line length [m]	835.5/ -	850.0/694.8	920.0/750.0
Anch./coupl. horizontal distance [m]	791.6/ -	796.9/640.0	858.5/640.0
Diameter of mooring chain [mm]	85	120	190
Mass of chain [kg/m]	138.1	275.2	690.0

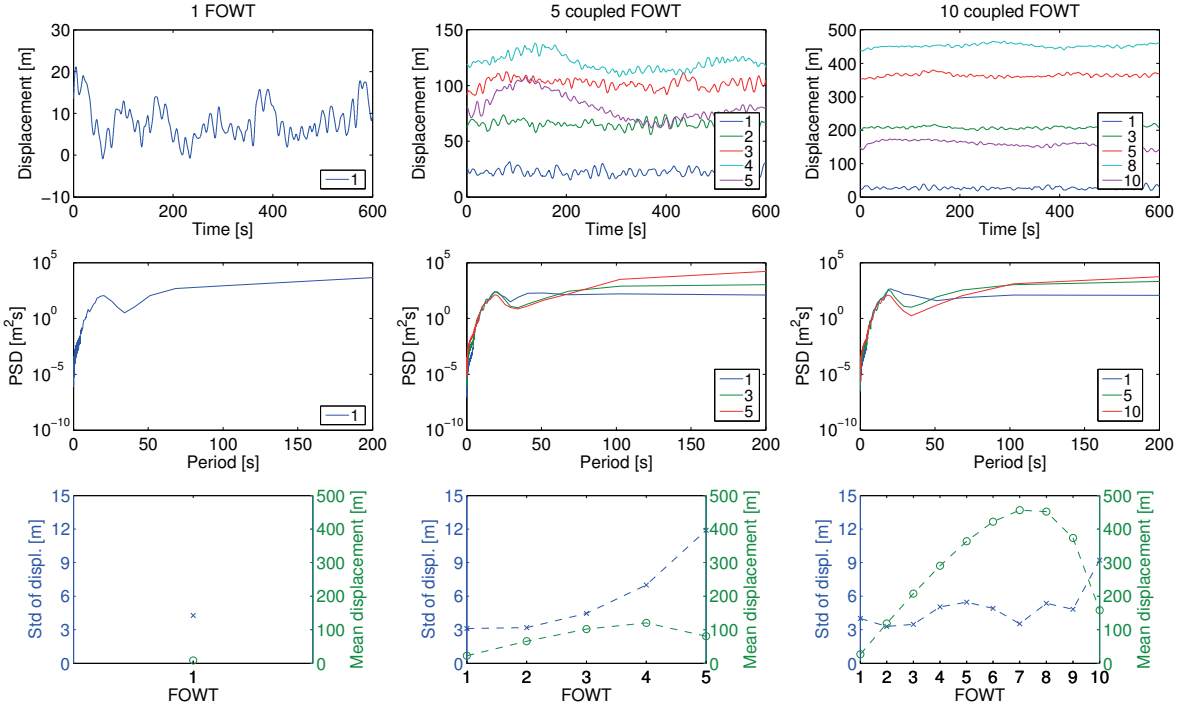

Fig. 4. Displacement time series, the corresponding power spectral densities, and standard deviations & mean values of displacements of row configurations with 1, 5 and 10 FOWTs for LC5 with H_S = 15.0m, T_P = 19.2s, v = 24ms^{-1}

and standard deviations and mean values are shown in the second and third row respectively. The displacements are measured against the global equilibrium position of each FOWT. In the displacement time series plots can be seen that the FOWTs are oscillating around positive mean displacements. While the displacements of the first floaters in coupled setups are only slightly larger than the displacements of the single floater, are the displacements of the following FOWTs in the coupled setups much larger and increasing with the number of the FOWT in the row until the 4th and 8th FOWT for the 5 and 10 coupled FOWT setups respectively. This is because the displacement is passed on to the following coupled FOWT as the mooring line force is depending on/a function of the horizontal distance between the coupled floaters. The displacements from the global equilibrium positions of the coupled FOWTs are large, with maximum displacements of ca. 135m and 475m for the 4th and 8th FOWT for the 5 and 10 coupled FOWT setups respectively. The displacements of FOWT(s) lying behind these floaters are decreasing. This can also be seen in the mean displacement plots in the third row of Fig. 4. The standard deviations, which are also shown in these plots lay around 3-4.5m for the single and first FOWTs of the coupled setups, and are increasing with the floater number to values around 12 and 9m for the last floaters of the coupled 5&10 floater setups respectively. The power spectral density curves for the single and 5&10 coupled FOWTs setups, shown in the second row of Fig. 4 have in general a similar shape for all FOWTs. The curves rise steeply to peak in wave period range, drop to local minima behind that, and then rise to their maxima in the low frequency range, except the curve of the first floater in the coupled setups, which flattens in the low frequency range. In the wave period range the curves of the first FOWTs in the coupled setups lie above the curves of last FOWTs. In the low frequency range, the curves of the last FOWTs in the coupled setups lie above the curves of the first FOWTs. In both cases the curves of the internal FOWTs falls in between the curves of the first and the last floaters. While first order wave period peaks are visible, no resonance seems to exist.

Some of the above observed effects can be understood employing Fig. 5. It shows time series of the deviation from the equilibrium distance between two neighboring floaters, or between the outside floaters and their anchors and the corresponding standard deviations and mean values. The distance deviation is defining the shape, stiffness and force of the mooring chain connecting neighboring FOWTs or a FOWT with an anchor. The lower and upper dashed horizontal lines indicate the distance where a taut line event for an outside anchored line or coupled line between two FOWTs would occur, respectively. The deviation curves that come closest to a taut line event and additional selected curves are shown. The FOWTs that lay at the beginning of coupled mooring systems (regarding the force direction) have increased horizontal distances and are closest to a taut event. The floaters at the end have decreased distances with a minimum down to -200m. This can be understood by considering the sum of the mean

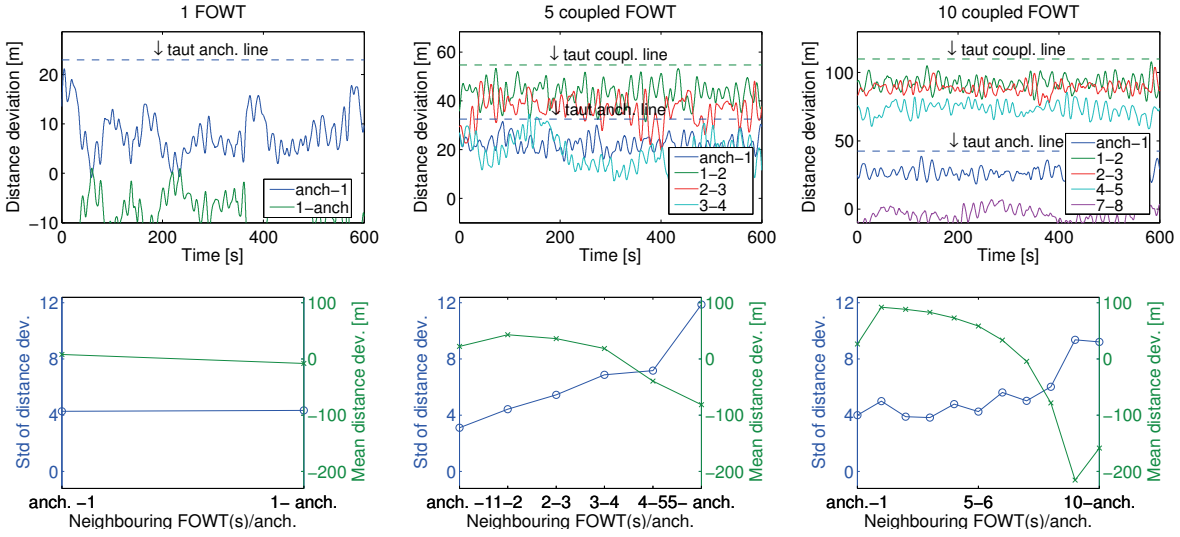

Fig. 5. Horizontal distance deviation between neighbouring floaters or a floater and an anchor (upper) and standard deviation and mean values of floater distance deviation (lower), for row configurations of 1, 5 and 10 FOWTs for LC5

force acting on each FOWT and how it is transferred to the anchors in the seabed. Due to the non-linear relationship between displacement and restoring force of catenary mooring lines, the force is strongly increased when the distance between the anchor and the fairlead is increased, while relatively slightly decreased when the distance is reduced in comparison. Hence, the first anchored mooring chain transfers the larger part of the environmental total mean force to the seabed, as the floaters at the beginning have increased distances resulting from the environmental forces. A smaller part of the force is set off due to the reduction of the mooring force from the last mooring chain that acts in line with the environmental force, as a result of the reduced distance between the last FOWT and its anchor. This may also be the reason for the increase in standard deviation with the floater number, as the stiffness of the mooring lines connected to the last floaters is decreased and lower restoring forces/a looser mooring system allow for larger dynamic displacements.

It is shown that coupled mooring systems are feasible in general as no dynamic phenomena like wave period resonance occur, however large displacements that appear in coupled mooring systems could be problematic considering the power cable connection to the FOWTs. The maintaining of an adequate distance to taut mooring lines or keeping the loads in the mooring chains below the breaking strength is challenging. Furthermore, the last floater (in force direction) in such a configuration comes relatively close to its anchor.

The dynamic response of the 5 floater row configuration to the operational load cases 1-4 is shown in Fig. 6 and 7. In general, similar behavior is observed, but motions occur in a smaller scale, with maximum displacements from 100 to 150m for the fourth FOWT as seen in the displacement time series and mean plots in the first row and third row of Fig. 6 respectively. The largest displacements are encountered at LC2, which is likely due to the large wind thrust force close to the rated wind speed. The power spectral density of the displacement in the second row does also show a similar behavior as observed in Fig. 4. The curves of the first floater lie below the curve of the first floater and the curve of the internal floater falls in between those curves. Only in the first load case the curve of the last and internal floater collapses. It can be seen that the low frequency response is of much larger magnitude and that the large wind thrust force close to rated wind speed in load case 2 leads to the largest response, which is also clarified by the mean displacement curves in the plots in the third row. The mean displacement and standard

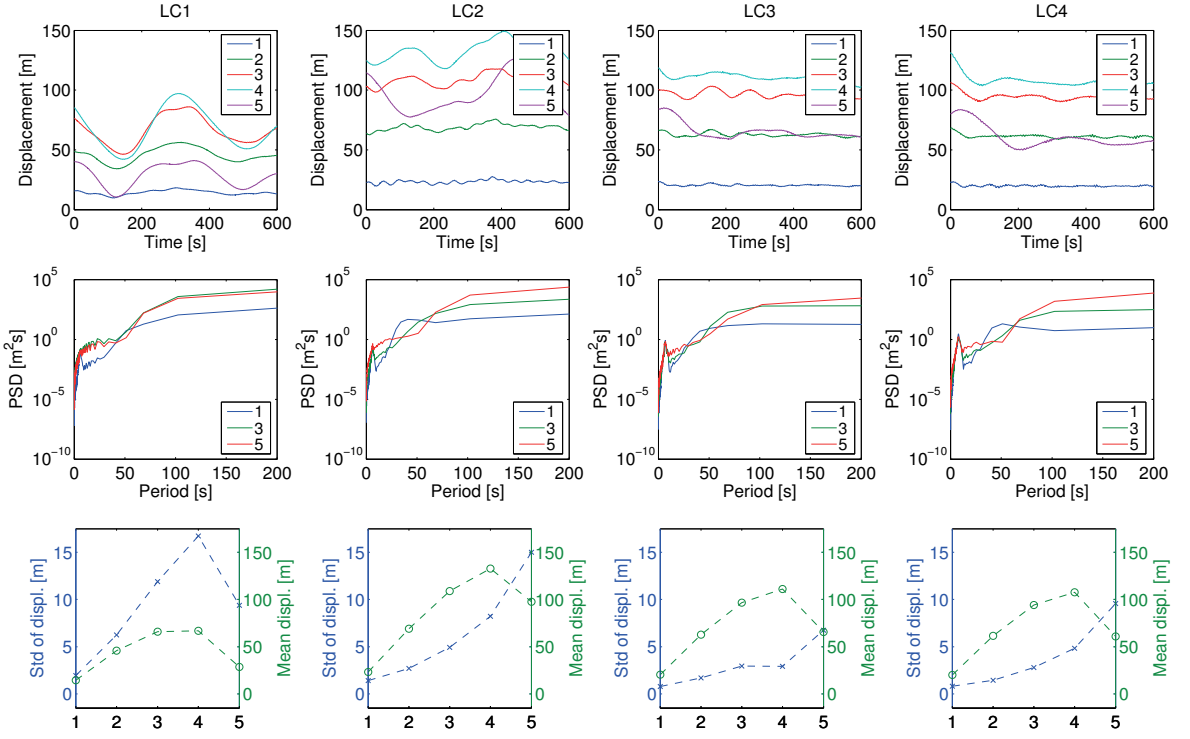

Fig. 6. Displacement time series (top), the corresponding power spectral densities (center), and standard deviations & mean values of displacements (bottom) of a row configuration with 5 floaters, operational load cases 1-4

deviations, shown in those plots, rise with increasing floater number, with exception of the decreasing mean displacements of the last floaters and the decreasing standard deviation of the last floater for LC1. The standard deviations of the first two load cases are higher compared to the load cases 3&4, however this might be due to a not fully settled system at that point.

The deviation of the equilibrium distance between two neighboring FOWT or between an outside floater and its anchor respectively, are shown in Fig. 7. The FOWTs are keeping in all operational load cases a safe distance to a taut event as seen in the first row, where the lower and upper dashed horizontal lines indicate the distance where an outside anchored line or coupled line between two FOWTs would become taut, respectively. The first and second FOWTs come closest to a taut event. That behavior has been already explained in the section before. In the second row the corresponding standard deviations and mean values are displayed. The standard deviations are in general increasing with the number of the floater in the row. The highest deviations are reached by the two last FOWTs in LC2 with ca. 13-15m. The mean values are in general decreasing with the floater number, but for the first floater.

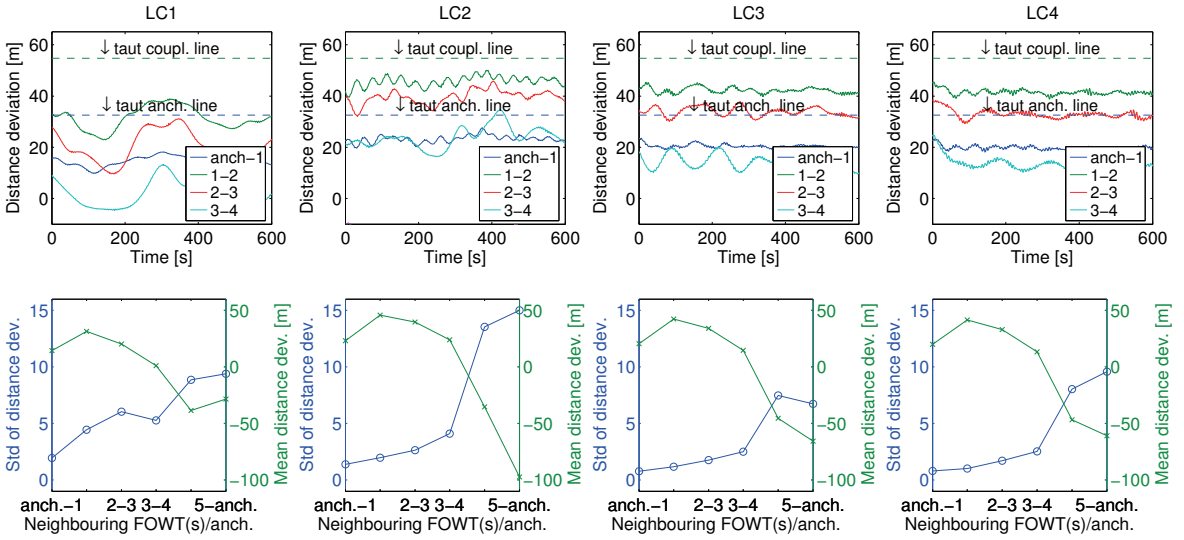

Fig. 7. Horizontal distance deviation between neighbouring floaters or a floater and an anchor (upper) and standard deviation and mean values of floater distance deviation (lower), of a row configuration with 5 floaters, operational load cases 1-4

3.3. Cost comparison

To estimate the saving potential of coupled catenary loose mooring systems a cost comparison with conventional catenary mooring systems is made. The proposed row, rectangular and triangular wind farm layouts are analysed. The conventional moored FOWTs used for comparison have the same number of mooring lines per floater corresponding to the coupled system layout (2, 3 and 4 mooring lines for the row, triangular and rectangular layout respectively), but each line is anchored to the seabed. The specific costs for the floating wind turbine, ancillaries, mooring lines and the costs for anchors are derived from a NREL report [10] where the economics floating wind turbine concepts are compared. The cost-comparison of coupled and conventional moored wind farms is shown in Fig. 3. The mooring chain diameters, length, costs, and

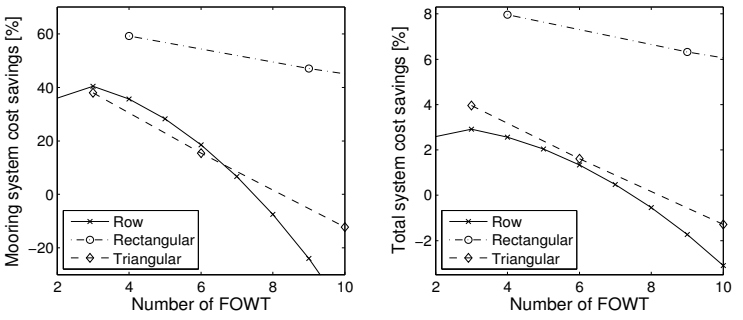

Fig. 8. Estimated mooring system and total system cost savings of coupled mooring systems (compared to conventional, non-coupled mooring systems with the same layout).

anchor costs for each layout corresponding to the total loading, which depends on the number of turbines in a coupled system, have been estimated based on the found values in Table 4.

Significant cost reductions of up to 60% in mooring system cost and 8% in total system cost can be achieved by using coupled mooring systems as shown in Fig. 8. The optima in savings lie at the smallest possible setups, with 3 or 4 floaters for the triangular and rectangular configurations respectively and at a number of 3 FOWTs for the row-layout. After that the saving rates are falling and become negative for the row and triangular setup at 8 and 10 FOWTs respectively, as the requirements due to loads in mooring chains and anchors and subsequent the costs increase with the number of FOWT in such systems. The maximum total system saving rates for row and triangular arranged layouts are 41% and 38% at a number of 3 FOWTs respectively. The total system cost savings are small in comparison; this is however due to the DeepC-platform that has a large share of the total system cost. Assuming a 25% share of mooring system cost 15%, 10.5% and 9.5% total system cost reductions could be achieved for rectangular, row and triangular arranged coupled systems respectively.

4. Discussion

The results are showing that coupled mooring systems are feasible considering the system dynamics and significant cost savings can be achieved. The analysis in the frequency domain indicated that no first-order wave force resonance problems would occur as the minimum natural periods of the different systems lie at 60s or higher. This was also confirmed by the time domain analysis of row-arranged layouts employing a one-dimensional simplified model where no first-order wave force resonance peaks did occur. However the displacements of FOWTs in coupled mooring systems can become large and are increasing with the number of FOWTs coupled, whereby the connection of a power cable may be difficult to realize. The requirements for the mooring system are increasing with the number of coupled floaters. The first anchored chain (in force direction) in such a system has to transfer the largest share of the load and the last floater comes relatively close to its anchor. The cost analysis showed that estimated cost reductions of up to 60% in mooring system costs and 8% in total system costs considering the DeepC-platform in a rectangular arranged coupled mooring system can be achieved. The optima in savings for the triangular and rectangular configurations lay at their smallest possible setups, with 3&4 FOWTs respectively. The row layouts optimum has been found for a number of 3 FOWTs. It should be noted that the simplified one-dimensional model for the row-arranged layout in the time domain disregards transverse motions; hence, the results and conclusions have to be taken with care. However, the row-layout is not considered a real world solution, as opposed to the triangular and rectangular layouts, but is more of theoretical interest as the simplified analysis of it is assumed to give a first insight of the dynamic behavior and problems coupled mooring systems may exhibit and if system cost reductions can be achieved. It should also be noted that mooring systems are usually designed specifically for each site and different configurations incl. different cable materials, clumped weights or buoys may lead to significantly differing results.

References

[1] Barltrop, N. D. P.: Floating structures: a guide for design and analysis. Bd. 101/98. Aberdeen: CMPT, 1998.
[2] Chakrabarti, Subrata K.: Handbook of offshore engineering. Amsterdam : Elsevier, 2005.
[3] Chakrabarti, Subrata K.: Steady drift force on vertical cylinder- viscous vs. potential. In: Applied ocean research 6 (1984), Nr. 2, p. 77
[4] Faltinsen, Odd M.: Sea loads on ships and offshore structures. Cambridge : Cambridge University Press, 1990. – VIII, 328 s
[5] Fischer, T. ; de Vries, W. ; Schmidt, B. : Upwind Design Basis (2010). Retrieved from repository.tudelft.nl, p. 116
[6] Fredriksson, David W. ; Decew, Judson C. ; Tsukrov, Igor ; Swift, M.R. ; Irish, James D. : Development of large fish farm numerical modelling techniques with in situ mooring tension comparisons, Aquacultural Engineering, volume 36 (2007), issue 2, p 137-148
[7] Gao, Z. ; Moan, T. : Mooring system analysis of multiple wave energy converters in a farm configuration, Paper presented at EWTEC 2009
[8] Luan, A. R. ; Jonkman, J. ; Masciola, M. ; Song, H. ; Goupee, A. ; Coulling, A. ; C.: Definition of the Semisubmersible Floating System for Phase II of OC4
[9] Matha, D. ; Schlipf, M. ; Cordle, A. ; Pereira, R. ; Jonkman, J. : Challenges in simulation of aerodynamics, hydrodynamics, and mooring-line dynamics of floating offshore wind turbines. National Renewable Energy Laboratory. 2011
[10] Musial, W. ; Butterfield, S. ; Boone, A.: Feasibility of Floating Platform Systems for Wind Turbines / National Renewable Energy Laboratory. 2004. – Research report
[11] Yamamoto, S. ; Colburn, W.E. Jr. : Power Generation Assemblies. International Patent, Publication Number W0 2005/040604 A2, 2005.